



Short communication

Hydrogen production on TiO₂ nanorod arrays cathode coupling with bio-anode with additional electricity generation



Qing-Yun Chen*, Jian-Shan Liu, Ya Liu, Yun-Hai Wang

State Key Laboratory of Multiphase Flow in Power Engineering, Xi'an Jiaotong University, Xianning Road, Xi'an 710049, PR China

H I G H L I G H T S

- A bio-photoelectrochemical cell is designed to produce hydrogen and electricity.
- Thermodynamic barrier of acetate to hydrogen is overcome without bias potential.
- The maximum hydrogen production of 4.4 $\mu\text{L h}^{-1}$ is achieved.

A R T I C L E I N F O

Article history:

Received 15 February 2013

Received in revised form

10 April 2013

Accepted 12 April 2013

Available online 19 April 2013

Keywords:

Microbial fuel cell

Microbial electrolysis cell

Acetate

Hydrogen

Semiconductor

A B S T R A C T

A novel microbial fuel cell with nanostructured TiO₂ semiconductor photocathode is designed with a proton exchange membrane to separate the anode chamber and the cathode chamber to overcome the thermodynamic barrier for hydrogen production from acetate without the aid of power supply. Hydrogen can be produced on n-type TiO₂ semiconductor photocathode with 0.2 mol L⁻¹ Na₂SO₄ as catholyte while acetate can be oxidized on bio-anode with additional electricity generated under light irradiation, spontaneously. With an external resistance of 10,000 Ω , the maximum power density of 6.0 mW m⁻² and the maximum hydrogen production rate of 4.4 $\mu\text{L h}^{-1}$ can be achieved. This design has potential application for the effective hydrogen production and provides a new method for utilization of the chemical energy in organic wastes by microbial fuel cells.

Crown Copyright © 2013 Published by Elsevier B.V. All rights reserved.

1. Introduction

Hydrogen, as an efficient renewable energy carrier, has attracted more and more attention due to the depletion of fossil fuels and the pollution caused by increasing energy demands [1,2]. Many techniques have been used to produce hydrogen, which include water electrolysis, photocatalytic water splitting, coal gasification, natural gas reforming and biomass fermentation [3]. Among them, photocatalytic water splitting using semiconducting photocatalysts has been considered as an environmentally friendly process for hydrogen production. However, the concentration of photo-generated electrons and holes is usually low, attributed to a high degree of recombination of electrons and holes, which decreases the photocatalytic efficiency [4]. Also organic or inorganic sacrificial

reagents are commonly used to enhance the hydrogen evolution rate [5].

Recently, microbial electrolysis cell (MEC), which derives from microbial fuel cell (MFC) utilizing bacteria to oxidize the biodegradable organics on bio-anode and releasing electrons to the cathode to form current, has been demonstrated to be a promising technique for hydrogen production from waste [6,7]. While for hydrogen production, a bias potential of 0.6 V or more has to be applied due to the thermodynamic barrier for hydrogen production on cathode and organics oxidation on anode [8,9]. The bias potential is usually supplied by a DC power source, which was not convenient for its application and required assistant electricity input. In order to overcome the thermodynamic barrier for hydrogen production without a DC power supply, researchers have tried to integrate photo energy harvesting component into the bio-electrochemical systems. Light assisted MEC operated with a photovoltaic cell to provide bias-potential has been reported [10,11]. In addition, Qian et al. investigated the coupling of p-type Cu₂O nanotube arrays photocathode with bio-anode and a

* Corresponding author. Tel./fax: +86 29 82665110.

E-mail addresses: qychen@mail.xjtu.edu.cn (Q.-Y. Chen), wang.yunhai@mail.xjtu.edu.cn (Y.-H. Wang).

considerable current enhancement was observed under light irradiation, but hydrogen evolution was not monitored [12]. Lu et al. reported the semiconductor mineral coated cathode coupling with the bio-anode [13]. However, the cathodic reaction was reduction of oxygen into water. To the best of our knowledge, there is no report on hydrogen production by coupling photocathode with bio-anode yet, especially by coupling with n-type semiconductor photocathode. The photocathode coupling with bio-anode for hydrogen production is worthy of further investigation.

Hence in the present work, we designed a novel microbial fuel cell by coupling an n-type nanostructured TiO₂ semiconductor photocathode with bio-anode to produce hydrogen and electricity spontaneously by consuming acetate substrate without DC power supply.

2. Experimental

2.1. Experimental apparatus

The schematic drawing of the bio-photoelectrochemical cell used in this research is shown in Fig. 1. As shown in Fig. 1, acetate is oxidized on the bio-anode with protons and electrons released. Protons can be transported to the cathode via an electrolyte, while electrons can be transferred to the cathode via the external circuit because under light irradiation the potential of the cathode can be higher than that of the anode. Thus, hydrogen can be produced on the photocathode. The electrochemical cell consists of two same-sized cylindrical chambers made of acrylic glass filled with anolyte and catholyte, respectively. Each of the chambers has a size of 3.2 cm in inner-diameter and 3.0 cm in length. There is one sampling hole for injecting and extracting water samples on the anode chamber. On the cathode chamber, there is one acrylic glass tube (25 mL free space) sealed by a rubber stopper for hydrogen collection and one quartz window sealed on the cathode cover for light irradiation. The two chambers are separated by a proton exchange membrane (PEM) (Nafion-117, Dupont). The anode is lab-made carbon fiber brush with Ti wire as current collector while the cathode is made of nanostructured TiO₂ nanorod arrays on conductive fluorine doped tin oxide coated (FTO) glass (2 cm × 1 cm) with copper foil as current collector.

2.2. Preparation and characterization of photocathode

TiO₂ nanorod arrays are synthesized by hydrothermal method. The expected solution for hydrothermal reaction is prepared by dissolving 4 mmol tetrabutyl titanate (TBOT) into 80 ml deionized water containing concentrated hydrochloric acid with stirring. This solution is put into 100 ml Teflon lined stainless steel autoclave.

After a cleaned and dried FTO is placed in the autoclave vertically, the autoclave is sealed and heated at 160 °C for 2 h in an oven. Then the as prepared TiO₂ nanorod arrays are rinsed with de-ionized water and heated at 400 °C in air for 0.5 h. Finally, the TiO₂/FTO electrodes are cut into 2 cm × 1 cm pieces and copper wires are attached to the electrodes using conductive silver glue, and then an epoxy resin is applied on the conductive silver glue layer to avoid unexpected conductive parts exposure to the electrolyte. The photocatalyst loading on each photoelectrode is c.a. 600 µg and the catalyst layer thickness is about 0.7 µm.

The morphology of the samples is determined by scanning electron microscopy (SEM) on JEOL JSM-6700F. The photocurrent was measured in a two chamber cell with 0.2 mol L⁻¹ Na₂SO₄ as electrolyte and Pt as counter electrode as described elsewhere [14,15]. The light source was provided by a 300W Xenon lamp (Beijing Trustech, China).

2.3. Start-up and operations

The anode is inoculated with sludge from an anaerobic reactor for fruit waste treatment. The anode medium consisted of acetate (1.6 g L⁻¹), NH₄Cl (0.31 g L⁻¹), NaH₂PO₄·2H₂O (5.18 g L⁻¹), Na₂HPO₄·12H₂O (6.15 g L⁻¹), KCl (0.13 g L⁻¹), other nutrients and vitamins added according to the previous report by other groups [16]. The bio-anode's start-up is in a single chambered MFC equipped with an air diffusion cathode as illustrated in other report [17]. During the anode inoculation, the anode and air cathode is connected via a 1000 Ω resistance till its voltage reaches a steady state of over 400 mV. After the maximum voltage reached, the external resistances of the MFC decreased from 1000 Ω–10 Ω step by step within 48 h and the MFC was operated with external resistance of 10 Ω for several weeks to obtain a stable voltage output. Then the anode is suitable to assemble with photocathode to build up the bio-photoelectrochemical cell as schematically shown in Fig. 1. The anode chamber is refilled with anode medium while the cathode chamber is refilled with 0.2 mol L⁻¹ Na₂SO₄. The cathode chamber is bubbled with N₂ for 15 min to remove residual oxygen in the catholyte and then the gas collection tube is sealed with a rubber stopper. In this stage, the bio-photoelectrochemical cell is ready for hydrogen and electricity production under light irradiation. The light source was the same as that for photocurrent measurement. The voltage is always monitored with a data logger (DAM-3059R, Beijing Art Technology Development Co. Ltd., China). The pH during the reaction is monitored with a pH meter (pHS-3C, Shanghai Leici Instruments, China).

2.4. Analysis

Hydrogen is extracted from the acrylic glass tube and its concentration is analyzed by a gas chromatography (SP-2100) equipped with a TCD detector with N₂ as carrier gas and NaX zeolite column. The power density and current output are calculated according to Eqs. (1) and (2):

$$P = U^2 / (R \cdot A) \quad (1)$$

$$I = U / R \quad (2)$$

Where P is the power density in W m⁻², I is the current flowing through the external circuit in A, U is the voltage across the resistor in V, R is the external resistance in Ω, and A is the apparent surface area of the photocathode equal to 2×10^{-4} m².

The cathode efficiency is defined as the percentage of hydrogen recovered from the current flowing through the external circuit (shown in Eq. (3)):

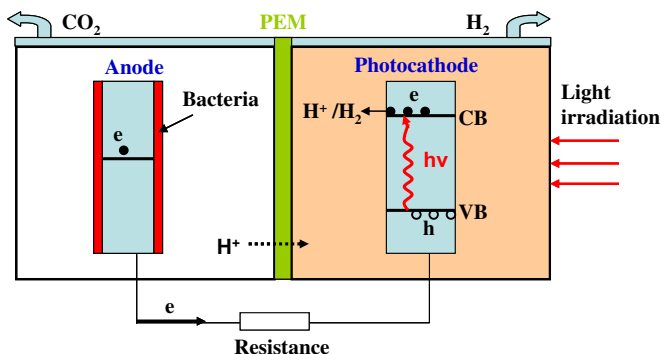


Fig. 1. Illustration for the bio-photoelectrochemical cell.

$$\eta_c = \frac{m_{H_2} * 96485}{\int_0^t i dt} * 100\% \quad (3)$$

Where i is the current transferred in μA and t is reaction time in seconds. m_{H_2} is the produced hydrogen amount in μg .

3. Results and discussions

3.1. Photocathode characterization

Fig. 2 shows the SEM image of the as-prepared photocathode. Obviously, TiO_2 nanorod arrays are successfully synthesized with a length of about 700 nm and a diameter of about 40 nm. As TiO_2 nanorod arrays grows vertically on the FTO substrate, they can provide a photogenerated electron direction path, with reduced crystal grain boundaries. The photocurrent of the TiO_2 electrode under light irradiation is shown in Fig. 3. The onset of the anodic photocurrent is around -0.8 V vs. SCE and increases sharply till 0.0 V vs. SCE. Then there appears a platform between 0.0 V and 1.0 V. This reveals that the TiO_2 arrays are loaded on the FTO plate uniformly with a good contact and the externally applied potential can promote the charge separation in the photoelectrochemical system.

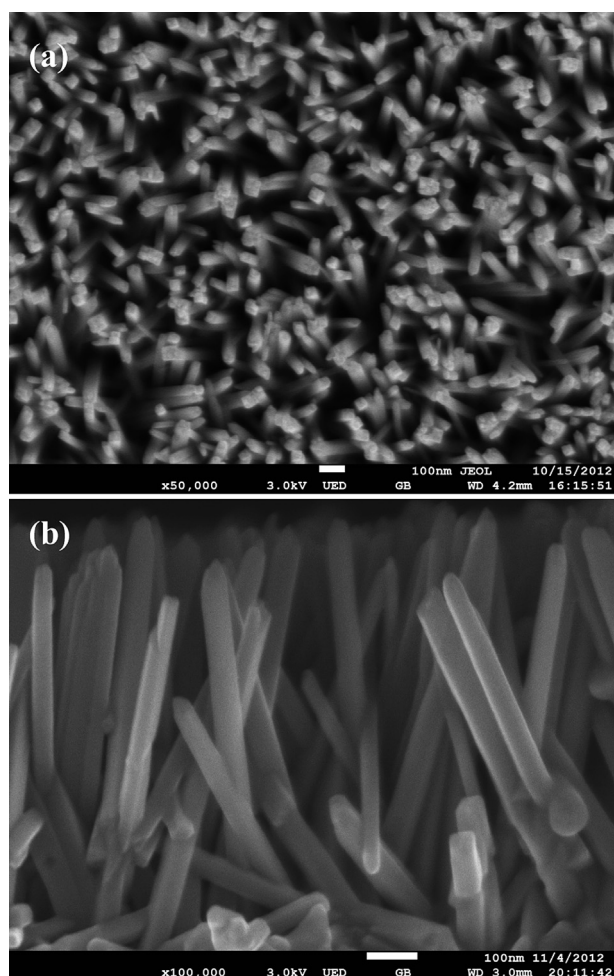


Fig. 2. SEM image of TiO_2 arrays: (a) top-view, (b) side-view.

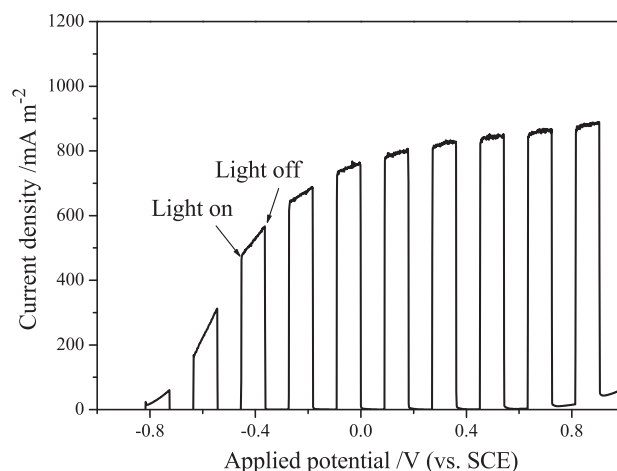


Fig. 3. I – V curve of TiO_2 electrode (electrolyte: $0.2 \text{ mol L}^{-1} \text{ Na}_2\text{SO}_4$, counter electrode: Pt foil.).

3.2. Electricity production performance

The present bio-photoelectrochemical cell is evaluated with and without light irradiation. As shown in Fig. 4, with external load of $10,000 \Omega$, the generated current density under light irradiation is about 50 – 55 mA m^{-2} , while without light irradiation the blank current density is only about 20 – 25 mA m^{-2} . It can be proposed that under light irradiation, the photocathode is activated to generate electron and hole pairs and makes the potential on the photocathode higher than that on the bio-anode. Thus the electrons released from acetate oxidation on the bio-anode are driven through the external circuit to the photocathode continuously. The electrons may reduce the protons to hydrogen on the photocathode. Some of them may also combine with the photogenerated holes on the photocathode.

In order to evaluate the electricity production performance of the present bio-photoelectrochemical cell, various external resistances are applied under light irradiation. The current and power output with different external resistance is recorded in Fig. 5. As shown in Fig. 5, the power density output shows a peak of 6.0 mW m^{-2} at external resistance of $10,000 \Omega$, which indicates the internal resistance of the present electrochemical cell with TiO_2 photocathode is around $10,000 \Omega$ under present irradiation

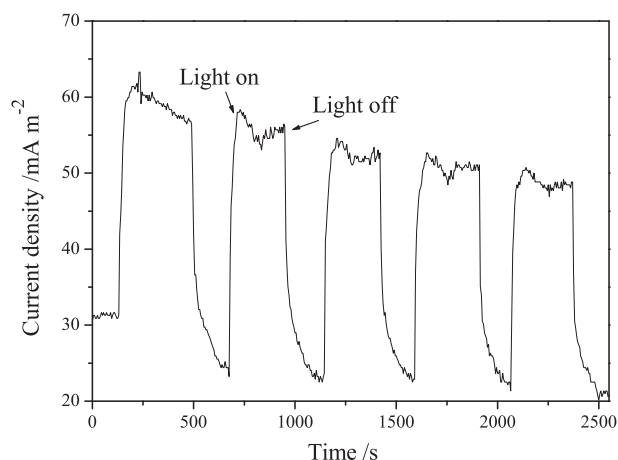


Fig. 4. Current density vs. time in MFC containing TiO_2 photocathode with and without light irradiation.

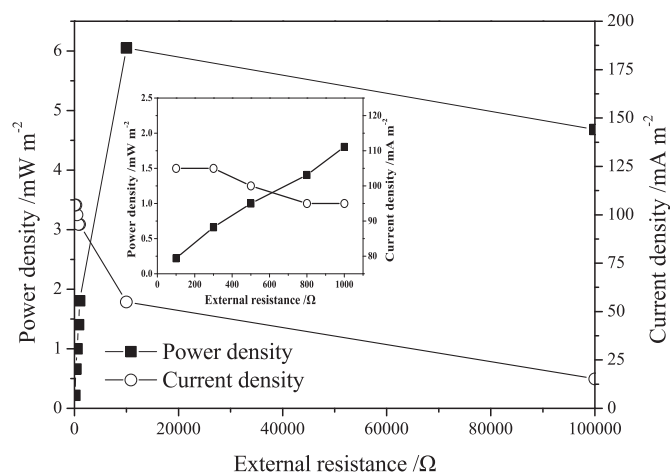


Fig. 5. Current density and power density output vs. external resistance (inset is the enlargement of the external resistance range of 100–1000 Ω).

condition. This internal resistance is much larger than traditional MFC and other electrochemical cell [18]. The large internal resistance may be derived from the resistance of the charge transfer on the photocathode, the semiconductor film on the cathode and the ions transportation through the PEM, etc. It can be expected that the internal resistance will be reduced by using a powerful irradiation or photocathode with a larger area. By using a thinner photocatalyst layer on photocathode may also help to decrease the internal resistance and enhance the electricity production. Reducing the cathodic pH would also help to increase the cathodic potential for hydrogen evolution. This may also help to improve the cell performance [19,20]. With acetate as anode substrate, the oxidation potential is usually about -0.28 V, while with glucose the anode potential can decrease to -0.42 V. The anodic potential decreasing may also help to improve the cell performance [6,7,21]. However, large internal resistance and low power density reveal that the present electrochemical cell might be not suitable for use as a power source directly before significant improvements are made. Furthermore, the current roughly increases with the external resistance decreasing as presumable phenomena. It is noted that the current reaches a platform when the external resistance decreases to 1000 Ω . The current density increases sharply from ca. 15 mA m^{-2} to 95 mA m^{-2} with the external resistance decreasing from 100,000 Ω to 1000 Ω . When the external resistance decreases further, the current density slightly increases to 105 mA m^{-2} . This also indicates the current limitation is possibly determined by the charge transfer on the photocathode.

3.3. Hydrogen production performance

Fig. 6 shows the hydrogen production versus the reaction time in a typical running. The typical running is done with an external resistance of 1000 Ω and the current density flowing through the external circuit is about 95 mA m^{-2} . The hydrogen amount increases steadily with the reaction time increasing. After 20 h reaction, the hydrogen amount reaches $87.7 \mu\text{L}$. The average hydrogen evolution rate of $4.4 \mu\text{L h}^{-1}$ is achieved in 20 h reaction time. That is $4.2 \text{ mL L}^{-1} \text{ d}^{-1}$ by normalizing the hydrogen production rate to the cathode chamber's volume (25 mL). This value is relative lower by comparing with MEC, for which the values are in the range of $0.01\text{--}6.3 \text{ L L}^{-1} \text{ d}^{-1}$ [6,22]. But it can be simply improved by decreasing the volume of cathode chamber in the present process. Thus we propose the hydrogen evolution rate without normalizing to the volume of cathodic chamber to be more

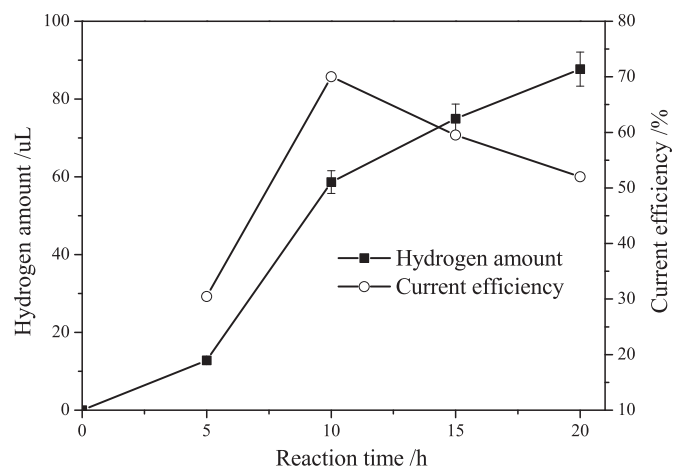


Fig. 6. Hydrogen production and current efficiency vs. reaction time in the photo-bioelectrochemical cell.

clearly and direct in Fig. 6. By using Eq. (3), the average current efficiency for hydrogen production in a certain time period is calculated and shown in Fig. 6. As shown in Fig. 6, the highest current efficiency of 70% is obtained at reaction time of 10 h while the lowest current efficiency of 30% is obtained at reaction time of 5 h. The current efficiency loss and variation may be due to the loss of hydrogen from penetration through the membrane or leakage. As previously reported [23,24] hydrogen diffusion through the membrane can occupy up to 67–94% of the total hydrogen amount. Thus, the loss of current efficiency shall be mainly due to the hydrogen monitoring. In addition, trace amount of oxygen can be monitored in the cathode chamber together with hydrogen which reveals that the photocatalytic water splitting process occurs by photo irradiation on TiO_2 electrode to produce hydrogen and oxygen. This photocatalytic water splitting process may result in a relative higher current efficiency because the hydrogen production via photocatalytic water splitting would not consume the electrons transferred from the external circuit. Though the hydrogen production rate is relative lower than that in a traditional MEC with similar size, it could be further improved by using such as a larger photocathode. Comparing with traditional photocatalytic water splitting technology, there are no sacrificial reagents needed and the recombination of photogenerated electrons and holes can be decreased. Therefore, this design has a potential application for the effective hydrogen production and provides a new method for utilization of the chemical energy in organic wastes by microbial fuel cells.

4. Conclusions

The n-type TiO_2 semiconductor photocathode is successfully coupled with bio-anode for hydrogen evolution and electricity production without bias-potential for the first time. The maximum power density of 6.0 mW m^{-2} is achieved in the present bio-photoelectrochemical cell. Hydrogen evolution rate of $4.4 \mu\text{L h}^{-1}$ is obtained on the TiO_2 cathode. The hydrogen evolution rate on the same catalyst loading is relative higher than that by photocatalytic water splitting. The present technology has a great potential for further improvement.

Acknowledgment

The National Basic Research Program of China (2009CB220000), Natural Science Foundation of China (NSFC) (Nos. 21206133 and

21206134) and doctoral program of Chinese Universities (20110201120042) supported the present research.

References

- [1] C.J. Winter, *Int. J. Hydrogen Energy* 34 (2009) S1–S2.
- [2] M. Sun, G.P. Sheng, Z.X. Mu, X.W. Liu, Y.Z. Chen, H.L. Wang, H.Q. Yu, *J. Power Source* 191 (2009) 338–343.
- [3] X.B. Chen, S.H. Shen, L.J. Guo, S.S. Mao, *Chem. Rev.* 11 (2010) 6503–6570.
- [4] S. Zhang, Q.Y. Chen, D.W. Jing, Y.H. Wang, L.J. Guo, *Int. J. Hydrogen Energy* 37 (2012) 791–796.
- [5] S.H. Shen, P.H. Guo, J.W. Shi, L.J. Guo, *Int. J. Nanotechnol* 8 (2011) 523–591.
- [6] H. Liu, S. Grot, B.E. Logan, *Environ. Sci. Technol.* 39 (2005) 4317–4320.
- [7] R.A. Rozendal, H.V.M. Hamelers, G.J.W. Euverink, S.J. Metz, C.J.N. Buisman, *Int. J. Hydrogen Energy* 31 (2006) 1632–1640.
- [8] D. Call, B.E. Logan, *Environ. Sci. Technol.* 42 (2008) 3401–3406.
- [9] B.E. Logan, D. Call, S. Cheng, H.V.M. Hamelers, T.J.H.A. Sleuteis, A.W. Jeremiasse, R.A. Rozendal, *Environ. Sci. Technol.* 42 (2008) 8630–8640.
- [10] K.J. Chae, M.J. Choi, K.Y. Kim, F.F. Ajayi, I.S. Chang, I.S. Kim, *Environ. Sci. Technol.* 43 (2009) 9525–9530.
- [11] F.F. Ajayi, K.Y. Kim, K.J. Chae, M.J. Choi, S.Y. Kim, I.S. Chang, I.S. Kim, *Int. J. Hydrogen Energy* 34 (2009) 9297–9304.
- [12] F. Qian, G.M. Wang, Y. Li, *Nano. Lett.* 10 (2010) 4686–4691.
- [13] A.H. Lu, Y. Li, S. Jin, H.R. Ding, C.P. Zeng, X. Wang, C.Q. Wang, *Energy and Fuels* 24 (2010) 1184–1190.
- [14] M. Li, J. Su, L. Guo, *Int. J. Hydrogen Energy* 33 (2008) 2891–2896.
- [15] M. Li, L. Zhao, L. Guo, *Int. J. Hydrogen Energy* 35 (2010) 7127–7133.
- [16] B.E. Logan, B. Hamelers, R. Rozendal, U. Schroder, J. Keller, S. Freguia, P. Aelterman, W. Verstraete, K. Rabaey, *Environ. Sci. Technol.* 40 (2006) 5181–5192.
- [17] A.T. Heijne, F. Liu, R.V. Weijden, J. Weijma, C.J. Buisman, H.V. Hamelers, *Environ. Sci. Technol.* 44 (2010) 4376–4381.
- [18] Y.Z. Fan, E. Sharbrough, H. Liu, *Environ. Sci. Technol.* 42 (2008) 8101–8107.
- [19] Y.H. Wang, B.S. Wang, Y.P. Liu, Q.Y. Chen, *Int. J. Hydrogen Energy* (2013), <http://dx.doi.org/10.1016/j.ijhydene.2013.03.043>.
- [20] G. Kyazze, A. Popov, R. Dinsdale, S. Esteves, F. Hawkes, G. Premier, A. Guwy, *Int. J. Hydrogen Energy* 35 (2010) 7716–7722.
- [21] P.A. Selembo, J.M. Perez, W.A. Lloyd, B.E. Logan, *Int. J. Hydrogen Energy* 34 (2009) 5373–5381.
- [22] B. Tartakovsky, M.F. Manuel, H. Wang, S.R. Guiot, *Int. J. Hydrogen Energy* 34 (2009) 672–677.
- [23] R.A. Rozendal, A.W. Jeremiasse, H.V.M. Hamelers, C.J.N. Buisman, *Environ. Sci. Technol.* 42 (2008) 629–634.
- [24] B.E. Logan, *Microbial Fuel Cells*, John Wiley & Sons, Inc., Hoboken, NJ, 2008.